

Angle-resolved photoemission study of the Ni(110)(1×2)-H reconstructed surface at 80 K

T. Komeda, Y. Sakisaka, and M. Onchi

Department of Chemistry, Faculty of Science, Kyoto University, Kyoto 606, Japan

H. Kato

Photon Factory, National Laboratory for High Energy Physics, Oho-machi, Ibaraki 305, Japan

S. Masuda

Department of Chemistry, College of Arts and Sciences, University of Tokyo, Komaba, Tokyo 153, Japan

K. Yagi

Institute of Physics, University of Tsukuba, Sakura-mura, Ibaraki 305, Japan

(Received 1 December 1986)

Angle-resolved photoemission spectroscopy utilizing synchrotron radiation has been used to study the electronic states of the Ni(110)(1×2)-H reconstructed surface at 80 K. An H-induced state, split off from the Ni bulk bands, is found at 9.0 eV below the Fermi energy at $\bar{\Gamma}$. This H split-off state disperses upwards by 3.1 eV with k_{\parallel} in the $[\bar{1}\bar{1}0]$ ($\bar{\Gamma}\bar{X}$) azimuth whereas it exhibits no measurable dispersion in the $[001]$ ($\bar{\Gamma}\bar{Y}'$) azimuth. The intrinsic Ni(110) surface states were not identified along the line in k space from $\bar{\Gamma}$ to \bar{X} . It was found that the $3d$ -like Σ_1 -symmetry bulk states at $\sim 2-3$ eV at $\bar{\Gamma}$ are markedly reduced by H adsorption, indicating that the Ni $3d$ (Σ_1) states participate in the bonding.

I. INTRODUCTION

In recent years, the dissociative adsorption of hydrogen on a Ni(110) surface at below ~ 180 K has been a subject of many experimental¹⁻⁶ and theoretical⁷⁻¹⁶ investigations. He diffraction¹ and low-energy electron diffraction^{2,3} (LEED) experiments have shown the formation of a sequence of hydrogen ordered phases for coverages (Θ) below one monolayer (ML), which are completed by a (2×1) -H phase at $\Theta=1$ ML. There is general agreement about the nature of these phases and their associated coverages;¹⁻³ the basic configuration is a zigzag $[\bar{1}\bar{1}0]$ row with H atoms in basically threefold sites on the embryonic (111). Above $\Theta=1$ ML, a reconstructed (1×2) phase grows continuously at the expense of the (2×1) phase until saturation is reached at $\Theta=1.5$ ML. For the (1×2) phase, possible structural models assuming the row-pairing type reconstruction of the substrate have been proposed [parts (a)-(c) of Fig. 1(A)]. The 1-ML H atoms still sit in the threefold-coordinated sites, and the additional $\frac{1}{2}$ -ML H atoms are adsorbed on the second Ni layer [on-top sites (a) (Ref. 1), bridge sites (b) (Refs. 1, 4, and 5) or buried in the fourfold-coordinated hollows with the (100) character (c) (Refs. 1-3)]. However, with the effort of several attempts,¹⁻⁶ no conclusive structural model has been derived for the (1×2) phase.

Previous theoretical workers have discussed the relative importance of the Ni sp and d orbitals in H chemisorption. However, there is still a controversy regarding this problem. Some concluded that the role of sp bonding is important (a minor role for d electrons),⁷⁻¹² and others

concluded that d bonding rather than sp bonding is important.¹³⁻¹⁶

The use of angle-resolved ultraviolet photoemission spectroscopy (ARUPS) can give valuable information about the nature of the chemisorption bond of H. Several ARUPS studies have been reported for H/Ti(0001),¹⁷ H/Pd(111),¹⁸ H/Pt(111),¹⁸ H/Ni(111),¹⁸ H/Ni(100),¹⁹ H/W(110),²⁰ H/Cu(111),²¹ and H/Ru(0001)²² and the two-dimensional band structure of the H-induced state (split-off state) was measured except for H/Ni(100) where such a split-off state failed to be observed¹⁹ (also see Refs. 23 and 24). Detailed measurement for H/Pd(111) (Ref. 18) showed that the bonding is predominantly H $1s$ -Pd $4d$ character. For H/Ni(110) a preliminary UPS study has been reported.³ In this paper, we report a detailed ARUPS study of the electronic states of the Ni(110)(1×2)-H surface at 80 K.

II. EXPERIMENTAL PROCEDURE

The Ni(110) single crystal was the same one used in our earlier experiments.^{25,26} The clean surface, showing the sharp $p(1\times 1)$ LEED pattern with a low background, was prepared by repeated Ar⁺-ion sputtering and annealing cycles. The amounts of impurities were reduced less than the detection limit of Auger spectroscopy [e.g., the Auger peak-height ratio, $I(O(KLL, 510 \text{ eV}))/I(Ni(LVV, 848 \text{ eV}))$, was less than $\frac{1}{400}$ and this corresponds to a coverage of 0.003 ML or less^{25,26}]. With liquid-N₂ cooling, the crystal could be cooled to ~ 80 K. The (1×2) -H reconstructed surface was prepared by exposing the clean

Ni(110) to hydrogen at $\sim 5 \times 10^{-8}$ Torr and at 80 K. The (1×2) -H structure was verified by LEED.

The ARUPS measurements using synchrotron radiation were performed at the sample temperature of 80 K using a 150° spherical-sector-type analyzer with an acceptance angle of $\pm 1^\circ$ as described elsewhere.^{25–28} The total experimental resolution was ~ 0.3 eV. The radiation was linearly polarized in the horizontal plane of incidence, and the sample was mounted onto a manipulator with one axis rotation and x, y, z translation such that the $[110]$ crystal azimuth was oriented horizontally. Therefore, throughout all the experiments, the surface component of the vector potential (\mathbf{A}) of the light was in the $[1\bar{1}0]$ azimuth (A_{\parallel} along $[1\bar{1}0]$). The electron energy analyzer was capable of angular motion in the (001) and $(1\bar{1}0)$ mirror planes, i.e., along the $[1\bar{1}0]$ ($\bar{\Gamma}\bar{X}$) and $[001]$ ($\bar{\Gamma}\bar{Y}'$) azimuths of the surface Brillouin zone (SBZ) for Ni(110)(1×2)-H [Fig. 1(B)]. The angle of light incidence, θ_i , from the surface normal could be varied independently. The base pressure in the system was 1×10^{-10} Torr. The parallel component of the detected electron momentum (k_{\parallel}) can be obtained directly from the measured kinetic energy (E_k) and its direction

$$k_{\parallel} = [(2m/\hbar^2)E_k]^{1/2} \sin\theta_e, \quad (1)$$

where θ_e is the emission angle in the collection plane measured from the surface normal.

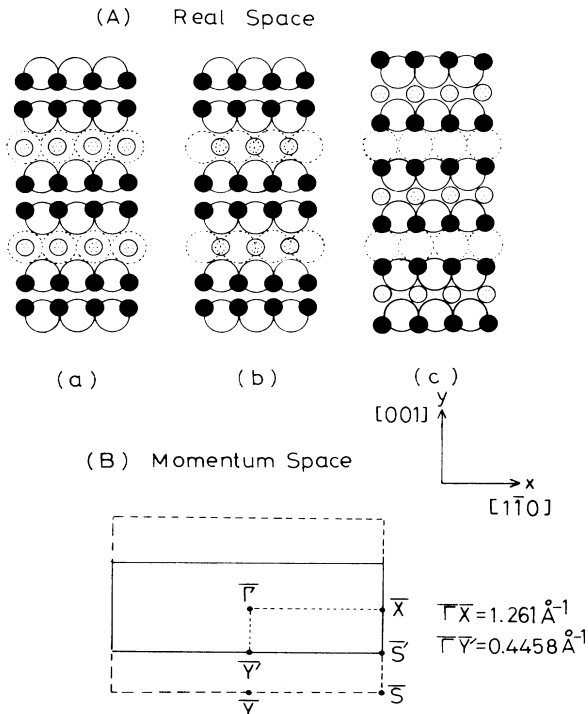


FIG. 1. (A) Structural models for Ni(110)(1×2)-H (Refs. 1–5). (B) Surface Brillouin zones for clean Ni(110) (dashed lines) and Ni(110)(1×2)-H (solid lines). The coordinate system is chosen such that the z axis is normal to the surface, and the x and y axes coincide with crystallographic $[1\bar{1}0]$ and $[001]$ directions, respectively.

III. RESULTS AND DISCUSSION

Figure 2 shows (a) normal-emission ($k_{\parallel}=0$ or $\bar{\Gamma}$) and (b) off-normal-emission spectra of the Ni(110)(1×2)-H surface measured at $\theta_i=60^\circ$ (A_{\parallel} along $[1\bar{1}0]$) and at various photon energies ($h\nu$). Binding energy is referred to E_F . All spectra in Fig. 2(b) were recorded at a fixed value of $k_{\parallel}=0.126 \text{ \AA}^{-1}$ in the $[1\bar{1}0]$ ($\bar{\Gamma}\bar{X}$) azimuth [i.e., $k_{\parallel}=\frac{2}{10}d(\bar{\Gamma}\bar{X})$ where $d(\bar{\Gamma}\bar{X})$ is the distance between $\bar{\Gamma}$ and \bar{X}] for an initial energy of 8.5 eV. In this way two-dimensional states can be identified; their energies in a spectrum should be independent of $h\nu$ if k_{\parallel} is held fixed. We find a new H-induced state, not present in the clean-surface spectra,^{25,26} at binding energies of 9.0 eV at $k_{\parallel}=0$ ($\bar{\Gamma}$) and ~ 8.5 eV at $k_{\parallel}=\frac{2}{10}d(\bar{\Gamma}\bar{X})$, as indicated by solid circles. The feature at ~ 6 eV is ascribed to the valence-band satellite in Ni which has been well investigated in Refs. 25 and 26. The centroid of this satellite shifts to ~ 7 eV at the Ni $3p$ -resonance ($h\nu_{\text{res}} \sim 68$ eV) as reported previously.^{25,26}

A more detailed picture of the electronic properties of the surface-adsorbate complex—i.e., characterization of

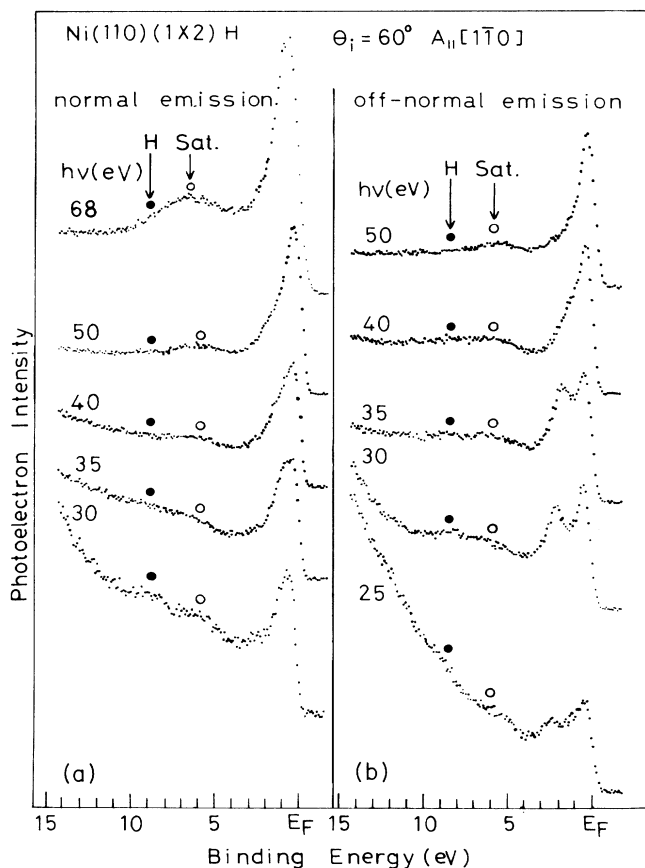


FIG. 2. $h\nu$ dependence of angle-resolved photoemission spectra for Ni(110)(1×2)-H taken at $\theta_i=60^\circ$ (A_{\parallel} along $[1\bar{1}0]$): (a) normal emission; (b) off-normal emission [$k_{\parallel}=\frac{2}{10}d(\bar{\Gamma}\bar{X})$ at 8.5 eV]. The peaks due to the H-induced bonding state are indicated by solid circles. The open circles indicate the position of the Ni valence-band satellite.

the adsorbate-substrate and adsorbate-adsorbate interactions—can be obtained by evaluating the E versus k_{\parallel} dispersion [$E(k_{\parallel})$] of the H-induced states. We have investigated the θ_e and $h\nu$ dependence of photoemission spectra for the clean Ni(110) and the Ni(110)(1 \times 2)-H in the two symmetry directions of the SBZ's (Figs. 3–5).

Before continuing with the discussion of the H-induced features, it is important to understand the off-normal-emission spectra for the clean surface. Figure 3 shows examples of such spectra for (a) $\theta_i = 60^\circ$ and (b) $\theta_i = 25^\circ$ (A_{\parallel} along $[1\bar{1}0]$), respectively, measured at $h\nu = 30$ eV and at emission angles $0^\circ \leq \theta_e \leq 16.4^\circ$ in the (001) mirror plane ($[1\bar{1}0]$ azimuth). The $\theta_i = 60^\circ$ spectra for larger emission angles are seen in Fig. 4 (left-hand side). The $h\nu$ dependence of the $\theta_e = 0^\circ$ spectra have been reported earlier^{25,26} and showed that at $\bar{\Gamma}$ (1) no features due to intrinsic surface states are observed, (2) the s -band emissions are so weak as to be detected for $25 \leq h\nu \leq 120$ eV, (3) the satellite moves with $h\nu$ as stated above, and (4) emissions from the $3d$ -like Σ_4 and Σ_1 bulk bands are observed, e.g., at ~ 0.5 and ~ 2.8 eV for $h\nu = 30$ eV, which move with $h\nu$ and the resulting experimental dispersion as well as locations of the bands agree well with the empirically adjusted band structure of Weling and Callaway.²⁹ Therefore, two features at ~ 0.5 and ~ 2.8 eV seen in $\theta_e = 0^\circ$ spectra of Fig. 3 are due to emissions from the $3d$ -like Σ_4 and Σ_1 bulk bands, respectively. These two peaks move in energy

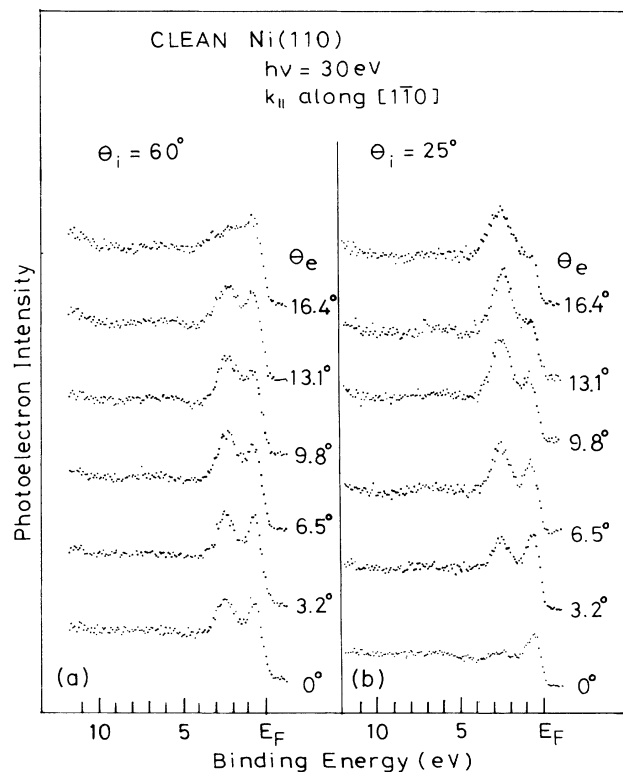


FIG. 3. Angle-resolved photoemission spectra of clean Ni(110) in the $\bar{\Gamma}\bar{X}$ ($[1\bar{1}0]$ azimuth) taken at $h\nu = 30$ eV (A_{\parallel} along $[1\bar{1}0]$) and at 80 K: (a) $\theta_i = 60^\circ$; (b) $\theta_i = 25^\circ$.

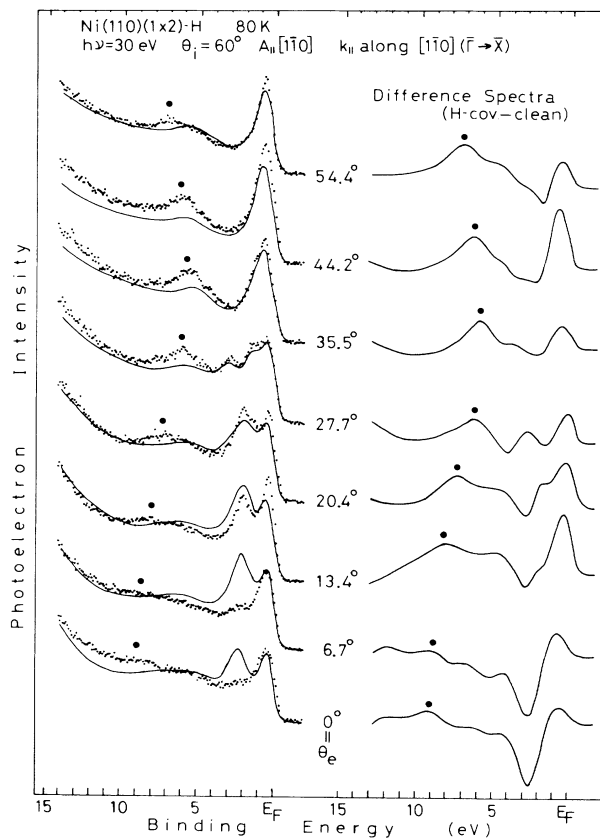


FIG. 4. Left-hand side: Angle-resolved photoemission spectra of Ni(110)(1 \times 2)-H at 80 K along $\bar{\Gamma}\bar{X}$ ($[1\bar{1}0]$) measured at $h\nu = 30$ eV and $\theta_i = 60^\circ$ (A_{\parallel} along $[1\bar{1}0]$). For comparison, the clean-surface spectra measured at the same experimental configuration are shown by solid lines. Right-hand side: Difference curves corresponding to the left-hand curves. The position of the H 1s derived state is indicated by solid circles.

as θ_e is changed. Note that the energy of the 6-eV satellite is independent of θ_e as expected. Figure 6(a) shows the measured dispersion along the $[1\bar{1}0]$ ($\bar{\Gamma}\bar{X}$) azimuth. The $h\nu = 30$ and 40 eV data are indicated by solid circles and triangles, respectively. The shaded regions in Fig. 6 are the calculated projection of the even-symmetry bulk bands onto the (110) surface Brillouin zone.³⁰ Clearly, the dispersion of the two $3d$ -band emissions obtained for $h\nu = 30$ eV differs from the dispersion for $h\nu = 40$ eV, indicating that these features are due to bulk states.

The dispersion profiles of the $3d$ bands in the clean Ni(110) surface taken at $h\nu = 30$ eV [Fig. 6(a)] are somewhat similar to the profiles for Ni(110) (Ref. 31) and Cu(110) (Ref. 32) obtained in the (001) mirror plane ($[1\bar{1}0]$ azimuth) at $h\nu = 21.2$ eV. The higher-binding-energy $3d$ -band peak starts to be split into two peaks at $\theta_e \sim 20^\circ$ for $h\nu = 30$ eV [Figs. 4 (left-hand side) and 6(a)]. The occurrence of this splitting is connected with the so-called appearance angle where the transition changes the final band in crossing a Bragg plane. From inspection of $\theta_i = 25^\circ$ spectra in Fig. 3(b) (predominantly A_{\parallel} along

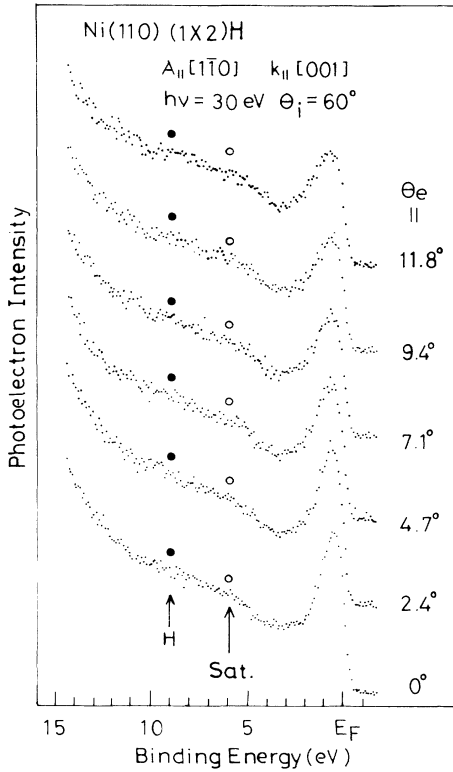


FIG. 5. Angle-resolved photoemission spectra along $\bar{\Gamma}\bar{Y}'$ ($[001]$) for Ni(110)(1 \times 2)-H measured at $h\nu=30$ eV and $\theta_i=60^\circ$ (A_{\parallel} along $[1\bar{1}0]$). The position of the H 1s derived state is indicated by solid circles. The open circles show the position of the Ni valence-band satellite.

$[1\bar{1}0]$ (x axis) and small A_z along $[110]$ (z axis)), we find that at $\theta_e \simeq 0^\circ$ the higher-binding-energy $3d$ -band peak is reduced in intensity as compared with the lower-binding-energy $3d$ -band peak, and at larger emission angles the former is increased in intensity as compared with the latter. According to the light polarization selection rules for direct transition, at $\theta_e \simeq 0^\circ$ the former is due to the transition $\Sigma_1(\text{initial}) \rightarrow \Sigma_1(\text{final})$ (allowed for z -polarized light) and the latter is due to $\Sigma_4 \rightarrow \Sigma_1$ transition (allowed for x -polarized light) as discussed in Refs. 25 and 26, while at larger emission angles the former and latter should be ascribed to the $\Sigma_1 \rightarrow \Sigma_4$ and $\Sigma_4 \rightarrow \Sigma_4$ transitions, respectively.

Now we turn to the two-dimensional dispersion of the H-induced features which is illustrated in the spectra in Figs. 4 and 5 and summarized in Fig. 6(b). Figures 4 (left-hand side) and 5 show off-normal-emission spectra of Ni(110)(1 \times 2)-H along the $[1\bar{1}0]$ ($\bar{\Gamma}\bar{X}$) and $[001]$ ($\bar{\Gamma}\bar{Y}'$) azimuths, respectively, taken at $h\nu=30$ eV and $\theta_i=60^\circ$ (A_{\parallel} along $[1\bar{1}0]$). Figure 4 (right-hand side) shows the difference curves [(1 \times 2)-H-clean] corresponding to the curves on the left-hand side. In principle, this eliminates the contribution from the underlying bulk interband transitions, and a positive peak in the difference curves indicates an extrinsic H-induced surface state, while a nega-

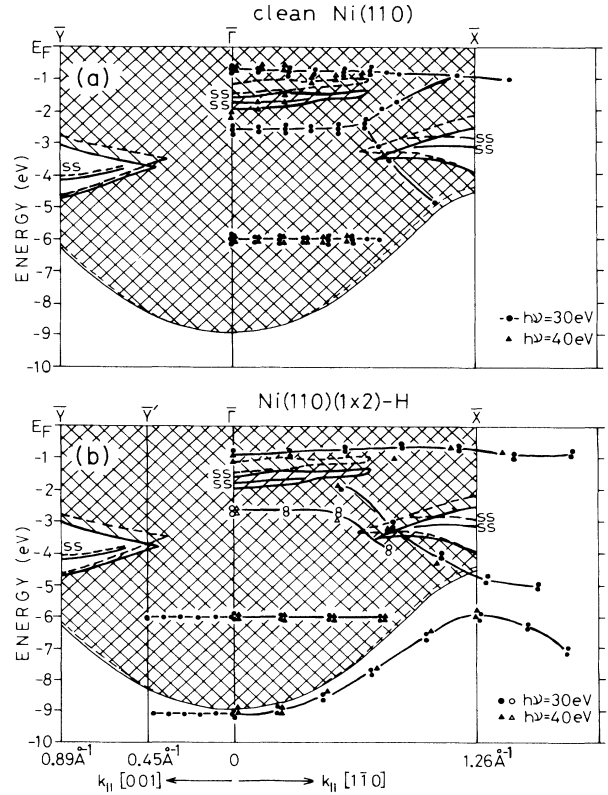


FIG. 6. Dispersion of the peaks in the photoemission spectra for (a) clean Ni(110) and (b) Ni(110)(1 \times 2)-H along $\bar{\Gamma}\bar{X}$ and $\bar{\Gamma}\bar{Y}'$ of the clean SBZ. The shaded regions are the calculated projection of the Ni bulk bands onto the (110) surface (Ref. 30); circles are for $h\nu=30$ eV and triangles are for $h\nu=40$ eV. The open symbols indicate negative peaks in the difference curves.

tive peak is an intrinsic Ni(110) surface state that has been removed or shifted by H adsorption. The feature due to the H 1s-Ni bonding state is indicated by solid circles. Notice that at and near $\bar{\Gamma}$ the higher-binding-energy Σ_1 symmetry $3d$ -band peak is reduced by H adsorption. This phenomenon is independent of $h\nu$ (see Fig. 2) and is therefore not due to final-state effects. Peak positions versus k_{\parallel} from series of off-normal-emission spectra for $h\nu=30$ eV (circles) and $h\nu=40$ eV (triangles) in the two symmetry directions $\bar{\Gamma}\bar{X}$ and $\bar{\Gamma}\bar{Y}'$ of the SBZ are shown in Fig. 6(b). There, the positions of peaks in the actual energy distribution curves and of positive peaks in the difference curves are indicated by solid symbols, while the positions of negative peaks in the difference curves are indicated by open symbols.

Here, it is important to note that H forms an ordered (1 \times 2) structure, and this fact makes the analysis of the angle-resolved difference curves difficult, because surface umklapp processes have been changed, and inelastic scattering from adsorbate has filled in minimum part in the clean-surface spectrum. Therefore, the difference curves may lead to several systematic errors and, as a

consequence, result in completely wrong interpretations. Criteria for identifying intrinsic or extrinsic surface state are (1) the structure is observed for several photon energies and (2) the structure is visible in the actual energy distribution curves, as well as in the difference curves. All the structures shown in Fig. 6(b) apparently satisfy the above criteria. However, a detailed comparison between Figs. 6(a) and 6(b) shows that, except for the H split-off states, dispersions of all the structures for Ni(110)(1×2)-H are almost identical with dispersions for clean Ni(110). In other words, no features due to intrinsic surface states are identified along $\bar{\Gamma}\bar{X}$, and the only extrinsic surface state unambiguously identified is the H 1s-Ni bonding split-off state. In the calculation of the clean surface,³⁰ the surface states were predicted at ~ 1.5 eV near $\bar{\Gamma}$ and at ~ 3 eV near \bar{X} . However, these surface states are not identified unambiguously in the present photoemission. Further, we do not find an H-induced state at ~ 1.3 eV below E_F as reported previously.³

Interestingly, the H split-off state does not exhibit dispersion in the [001] ($\bar{\Gamma}\bar{Y}'$) azimuth, though it shows considerable dispersion of ~ 3.1 eV in the [1 $\bar{1}$ 0] ($\bar{\Gamma}\bar{X}$) azimuth, i.e., parallel to the densely packed rows of the H atoms [see Fig. 1(A)]. The dispersion along $\bar{\Gamma}\bar{X}$ is characteristic of an *s*-derived orbital and exhibits the correct periodicity for the (1×2) structure. The lack of dispersion in this state along $\bar{\Gamma}\bar{Y}'$ may be a consequence of the complicated periodicity of the (1×2)-H structure in the [001] azimuth. We think that the visible split-off state is for H in a basically threefold-coordinated site and/or at the second Ni layer for the following reason. No split-off state was found¹⁸ for H adsorption on Ni(100) surface at 90 K, and therefore the visible split-off state is not expected for H in the fourfold-coordinated hollow with the (100) character [part (c) of Fig. 1(A)]. It has been suggested that the H-metal bonding is short-ranged and hardly extends beyond the nearest neighbors.¹⁶ These results show that unfortunately it is impossible to decide which structural model is correct from photoemission data alone.

As shown in Fig. 2, the H 1s-Ni split-off state is most visible at around $h\nu=30$ eV. This indicates a strong admixture of Ni 3*d* states into this split-off level, because the photoionization cross section for atomic H 1s slowly decreases as $h\nu$ increases and the Hartree-Fock calculations show that atomic Ni 3*d* cross-section peaks at 20–34 eV.³³ There seems to be more direct evidence for strong hybridization with Ni 3*d* states. As stated above, we find that Σ_1 -symmetry 3*d* bulk states are almost completely removed by H adsorption, irrespective of $h\nu$ (see Fig. 4). The H 1s orbitals interact with Ni states which belong to the same irreducible representations to form the split-off bonding state. It has been pointed out³⁴ that the contributions of surface and bulk states to the chemisorption bond are expected to be similar.

Figures 4 and 5 show that the H split-off state is more pronounced away from $\bar{\Gamma}$. The same phenomenon has also been observed on Ni(111) (Ref. 18) and Ru(0001) (Ref. 22) and was explained by theoretical results¹⁶ that the *d* character of the split-off state increases for the outer part of the SBZ. However, contrary to what was tacitly

assumed, the atomic H 1s cross section is not much weaker than the Ni 3*d* cross section per electron at $h\nu\sim 20$ –30 eV, but they are much the same.^{33,35,36} Therefore, there is still a problem with the above explanation. Another explanation, i.e., an Anderson-Newns type initial-state broadening,¹³ for this reduction in intensity of the H split-off state around $\bar{\Gamma}$ was offered. At $\bar{\Gamma}$ the H split-off state is only 0.2 eV off from the Ni *s* bulk bands, and this state has the measured width [full width at half maximum] of ~ 1.5 eV near the zone boundary where it is well separated from the bottom of the *s* bands [see Fig. 6(b)]. Since at $\bar{\Gamma}$ the split-off state is very close to the bulk *s*-band edge and then almost overlaps the *s* band, it can acquire an additional width, making it broader. We cannot reject this explanation.

Finally, we want to discuss lateral interactions for hydrogen ordered overlayers. When the average H-H spacing decreases, the magnitude of the dispersion is expected to increase from a simple tight-binding-model argument for an "isolated" monolayer. The implication of this model is that the band dispersion is primarily a consequence of direct ("through-space") H-H interactions and not due to indirect interactions through the substrate. Within this simple picture the bandwidth (E_{BW}) depends exponentially on the H-H nearest-neighbor distance (d). Figure 7 shows a compilation of the available experimen-

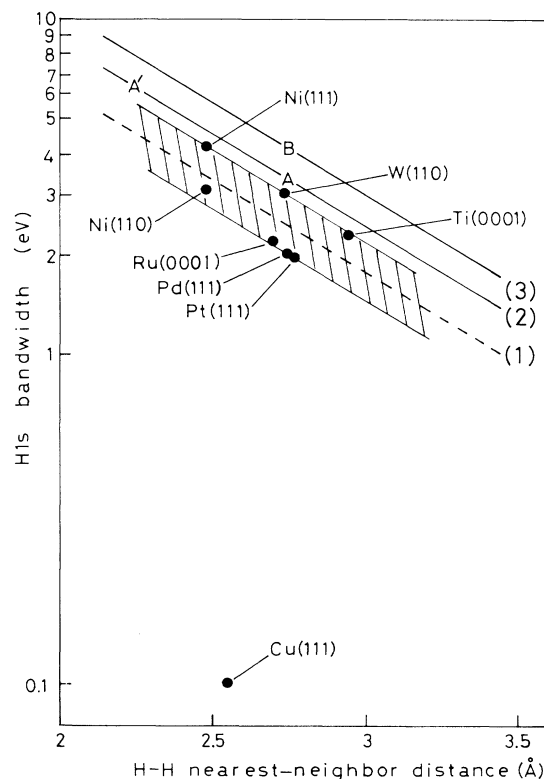


FIG. 7. Bandwidth of the H split-off state versus H nearest-neighbor distance on Ni(110)(1×2)-H (this work), Ti(0001)(1×1)-H, (Ref. 17), Ni(111)(1×1)-H (Ref. 18), Pd(111)(1×1)-H (Ref. 18), Pt(111)(1×1)-H (Ref. 18), W(110)(1×1)-H (Ref. 20), Cu(111)(1×1)-H (Ref. 21), and Ru(0001)(1×1)-H (Ref. 22) surfaces, in a semilog plot (see text).

tal data for the H 1s bandwidth as a function of the H-H distance [for Ni(111) and Pd(111),¹⁸ the values in the $\bar{\Gamma}\bar{K}$ azimuths in the SBZ's of hexagonal overlayers are plotted]. The straight line (1) corresponds to an exponential decay constant of $\sim 0.8 \text{ \AA}$, i.e., the bandwidth E_{BW} is approximately given by

$$E_{\text{BW}} = 75.8e^{-d/0.803}, \quad (2)$$

where E_{BW} is in eV and d is in \AA . The additional substrate interaction, which depends on the realistic bulk band structure of the substrate, leads to a deviation from the exponential relation between E_{BW} and d . Although the data in Fig. 7 are considerably scattered, the general trend of the data indicates that, except for H/Cu(111),³⁷ the bandwidth of the H 1s split-off state seems to be roughly determined by the H-H distance.

Theoretically, a few calculations of the band structure for a hydrogen monolayer have been reported.^{38,39} For an isolated monolayer of hydrogen with lattice spacing corresponding to the $p(1 \times 1)$ overlayer on Pd(111) ($\Theta=1$ ML), the H 1s bandwidth in the $\bar{\Gamma}\bar{M}$ and $\bar{\Gamma}\bar{K}$ azimuth are calculated to be ~ 3.4 and 4.2 eV, respectively:³⁸ the values are indicated by A and B in Fig. 7. Similar calculation for an isolated hydrogen monolayer with lattice spacing corresponding to the $p(1 \times 1)$ overlayer on $W(100)$ ($\Theta=2$ ML) gives the H 1s bandwidth of ~ 3.2 eV in the $\bar{\Gamma}\bar{X}$ azimuth.³⁹ This dispersion is half magnitude of the dispersion in a hexagonal layer along $\bar{\Gamma}\bar{M}$ for the same H-H spacing (see Ref. 40). Therefore, in this case, the corrected value is indicated in Fig. 7 by A' . The straight line (2) connecting A with A' has nearly the same slope as the line (1). The line (3) is a straight line passing through B which has the same slope as the line (2). We assume that the lines (2) and (3) can give the bandwidths in the $\bar{\Gamma}\bar{M}$ and $\bar{\Gamma}\bar{K}$ azimuths, respectively, for an isolated hexagonal hydrogen monolayer. Note that the experimental H 1s bandwidth is smaller than the theoretical bandwidth obtained for the isolated hydrogen monolayer. This fact as well as the above-mentioned certain deviations of the experimental data from the simple exponential relation between E_{BW} and d indicate that the additional through-substrate interaction is also operative.

The avoided-level-crossing mechanism has been proposed^{18,38} to explain the small bandwidth observed in photoemission from the Pd(111)(1 \times 1)-H surface. This mechanism could be qualitatively possible for the Pd(111)(1 \times 1)-H system, since the energy difference (ΔE) between the bottom of the substrate d -like bulk bands at M or K and the H 1s level at $\bar{\Gamma}$ is below the line (2) or (3). However, we cannot predict easily the bandwidth by this idea without realistic band-structure calculation, and it is unknown whether this mechanism is operative for the other adsorption systems. For example, in the case of the

Ni(111)(1 \times 1)-H system, the ΔE values are estimated to be ~ 5.9 eV at \bar{K} and ~ 5.4 eV at \bar{M} from the results of Refs. 18 and 41, and they are above the respective lines (2) and (3). Therefore, we can expect to observe the full bandwidths given by the lines (2) and (3) contrary to experiment [the observed E_{BW} in the $\bar{\Gamma}\bar{M}$ azimuth is ~ 3.2 eV (Ref. 18)]. Similar argument holds for the Ti(0001)(1 \times 1)-H system [$\Delta E \simeq 5.5$ eV (Ref. 17)]. At best, the avoided level crossing model can give only a possible upper limit of bandwidth. We can expect the H 1s bandwidth using the empirical formula (2) within an error of ~ 0.5 eV for $d \leq 2.5 \text{ \AA}$. Of course, this does not exclude the indirect interaction, as discussed above. The underlying physics of the avoided-level-crossing model is that the hydrogen-substrate hybridization can be an important factor responsible for the observed bandwidth. Another essential parameter characterizing the bandwidth is the H-H distance. The problem is attributed to the choice of the wave function of adsorbed hydrogen including hybridization. We can say that hydrogen-substrate hybridization makes the hydrogen bandwidth decrease. This point requires further study.

IV. CONCLUDING REMARKS

Angle-resolved photoemission measurements have been made on clean Ni(110) and Ni(110)(1 \times 2)-H surfaces at 80 K. No features due to the intrinsic surface states were identified along $\bar{\Gamma}\bar{X}$, while the H 1s derived bonding level split off from the bulk bands was found (9.0 eV at $\bar{\Gamma}$). This split-off state shows no measurable dispersion along $\bar{\Gamma}\bar{Y}'$ ([001]), whereas it exhibits considerable dispersion of ~ 3.1 eV along $\bar{\Gamma}\bar{X}$ ([1 $\bar{1}$ 0]). These results reflect the highly anisotropic structure of the (1 \times 2)-H. We found evidence for participation of the Ni Σ_1 -symmetry $3d$ -like bulk bands in the H-Ni bonding.

We did not study the low-coverage phases [i.e., (2 \times 6), $c(2 \times 4)$, and (2 \times 1)], since postadsorption of hydrogen from the background can change a particular phase to another phase during the period of ~ 1 h for carrying out a series of measurements. Further experiments will have to be carried out.

ACKNOWLEDGMENTS

The experiments were performed at the Photon Factory, National Laboratory for High Energy Physics, Japan. We are pleased to thank the staffs of Photon Factory, particularly T. Miyahara, for their excellent support. We wish to thank Y. Aiura for his assistance during experiment. This work was supported in part by the Grant-in-Aid for Scientific Research from the Ministry of Education.

¹K. H. Rieder and W. Stocker, Surf. Sci. **164**, 55 (1985).

²V. Penka, K. Christmann, and G. Ertl, Surf. Sci. **136**, 307 (1984).

³K. Christmann, F. Chehab, V. Penka, and G. Ertl, Surf. Sci.

152/153, 356 (1985).

⁴M. Jo, M. Onchi, and M. Nishijima, Surf. Sci. **154**, 417 (1985).

⁵L. Ollé and A. M. Baró, Surf. Sci. **137**, 607 (1984).

⁶N. J. DiNardo and E. W. Plummer, Surf. Sci. **150**, 89 (1985).

- ⁷G. Blyholder, *J. Chem. Phys.* **62**, 3193 (1975).
- ⁸D. J. M. Fassaert and A. van der Avoird, *Surf. Sci.* **55**, 291 (1976).
- ⁹C. F. Melius, J. W. Moskowitz, A. P. Mortola, M. B. Baillie, and M. A. Ratner, *Surf. Sci.* **59**, 279 (1976).
- ¹⁰R. P. Messmer, D. R. Salahub, K. H. Johnson, and C. Y. Yang, *Chem. Phys. Lett.* **51**, 84 (1977).
- ¹¹T. H. Upton and W. A. Goddard III, *Phys. Rev. Lett.* **42**, 472 (1979).
- ¹²P. Nordlander, S. Holloway, and J. K. Nørskov, *Surf. Sci.* **136**, 59 (1984).
- ¹³J. P. Muscat and D. M. Newns, *Phys. Rev. Lett.* **43**, 2025 (1979).
- ¹⁴R. Dovesi, C. Pisani, and C. Roetti, *Surf. Sci.* **103**, 482 (1981).
- ¹⁵M. Weinert and J. W. Davenport, *Phys. Rev. Lett.* **54**, 1547 (1985).
- ¹⁶C. T. Chan and S. G. Louie, *Phys. Rev. B* **30**, 4153 (1984).
- ¹⁷P. J. Feibelman, D. R. Hamann, and F. J. Himpsel, *Phys. Rev. B* **22**, 1734 (1980).
- ¹⁸W. Eberhardt, F. Greuter, and E. W. Plummer, *Phys. Rev. Lett.* **46**, 1085 (1981); W. Eberhardt, S. G. Louie, and E. W. Plummer, *Phys. Rev. B* **28**, 465 (1983); F. Greuter, I. Strathy, E. W. Plummer, and W. Eberhardt, *ibid.* **33**, 736 (1986).
- ¹⁹P. A. Dowben and Y. Sakisaka (unpublished).
- ²⁰G. B. Blanchet, N. J. DiNardo, and E. W. Plummer, *Surf. Sci.* **118**, 496 (1982).
- ²¹F. Greuter and E. W. Plummer, *Solid State Commun.* **48**, 37 (1983).
- ²²P. Hofmann and D. Menzel, *Surf. Sci.* **152/153**, 382 (1985).
- ²³H. Kato, Y. Sakisaka, M. Nishijima, and M. Onchi, *Phys. Rev. B* **22**, 1709 (1980).
- ²⁴H. Kato, Y. Sakisaka, M. Nishijima, and M. Onchi, *Surf. Sci.* **107**, 20 (1981).
- ²⁵Y. Sakisaka, T. Komeda, M. Onchi, H. Kato, S. Masuda, and K. Yagi, *Phys. Rev. Lett.* **58**, 733 (1987).
- ²⁶Y. Sakisaka, T. Komeda, M. Onchi, H. Kato, S. Masuda, and K. Yagi (unpublished).
- ²⁷H. Kato, T. Ishii, S. Masuda, Y. Harada, T. Miyano, T. Komeda, M. Onchi, and Y. Sakisaka, *Phys. Rev. B* **32**, 1992 (1985).
- ²⁸Y. Sakisaka, T. Komeda, T. Miyano, M. Onchi, S. Masuda, Y. Harada, K. Yagi, and H. Kato, *Surf. Sci.* **164**, 220 (1985).
- ²⁹F. Weling and J. Callaway, *Phys. Rev. B* **26**, 710 (1982).
- ³⁰D. G. Dempsey, W. R. Grise, and L. Kleinman, *Phys. Rev. B* **18**, 1270 (1978).
- ³¹H. Mårtensson and P. O. Nilsson, *Phys. Rev. B* **30**, 3047 (1984).
- ³²R. Courths, V. Bachelier, B. Cord, and S. Hufner, *Solid State Commun.* **40**, 1059 (1981).
- ³³F. Combet-Farnoux and M. Ben Amar, *Phys. Rev. A* **21**, 1975 (1980).
- ³⁴T. B. Grimley, in *The Nature of the Surface Chemical Bond*, edited by T. N. Rhodin and G. Ertl (North-Holland, Amsterdam, 1979).
- ³⁵D. A. L. Kilcoyne, C. M. McCarthy, S. Nordholm, N. S. Hush, and P. R. Hilton, *J. Electron Spectrosc. Relat. Phenom.* **36**, 153 (1985).
- ³⁶E. J. McGuire, *Phys. Rev.* **175**, 20 (1968); Sandia Laboratories (Albuquerque, NM) Research Report No. SC-PR-70-721 (1970).
- ³⁷For this system, the overlayer structure has not been confirmed by LEED, and therefore there is high ambiguity in determining the value of d .
- ³⁸S. R. Chubb and J. W. Davenport, *Phys. Rev. B* **31**, 3278 (1985).
- ³⁹R. Richter and J. W. Wilkins, *Surf. Sci.* **128**, L190 (1983).
- ⁴⁰F. Greuter, D. Heskett, E. W. Plummer, and H. J. Freund, *Phys. Rev. B* **27**, 7117 (1983).
- ⁴¹W. Eberhardt and E. W. Plummer, *Phys. Rev. B* **21**, 3245 (1980).